



Light polarization sensitive photodetectors with m- and r-plane homoepitaxial ZnO/ZnMgO quantum wells

G. Tabares, A. Hierro, M. Lopez-Ponce, E. Muñoz, B. Vinter, and J.-M. Chauveau

Citation: [Applied Physics Letters](#) **106**, 061114 (2015); doi: 10.1063/1.4908183

View online: <http://dx.doi.org/10.1063/1.4908183>

View Table of Contents: <http://scitation.aip.org/content/aip/journal/apl/106/6?ver=pdfcov>

Published by the [AIP Publishing](#)

Articles you may be interested in

[Monolithic color-selective ultraviolet \(266–315nm\) photodetector based on a wurtzite \$Mg_xZn_{1-x}O\$ film](#)
Appl. Phys. Lett. **105**, 133510 (2014); 10.1063/1.4897300

[Low-threshold lasing action in an asymmetric double ZnO/ZnMgO quantum well structure](#)
Appl. Phys. Lett. **103**, 131104 (2013); 10.1063/1.4822265

[Lattice strains and polarized luminescence in homoepitaxial growth of a-plane ZnO](#)
Appl. Phys. Lett. **101**, 231901 (2012); 10.1063/1.4769036

[Polarization-sensitive Schottky photodiodes based on a-plane ZnO/ZnMgO multiple quantum-wells](#)
Appl. Phys. Lett. **99**, 071108 (2011); 10.1063/1.3624924

[Low temperature reflectivity study of nonpolar ZnO/\(Zn,Mg\)O quantum wells grown on M-plane ZnO substrates](#)
Appl. Phys. Lett. **98**, 101913 (2011); 10.1063/1.3565969

A banner for Applied Physics Letters featuring the journal's logo and the text "Meet The New Deputy Editors". Below the text are three circular headshots of the new deputy editors: Alexander A. Balandin, Qing Hu, and David L. Price.

AIP | Applied Physics Letters

Meet The New Deputy Editors

 Alexander A. Balandin

 Qing Hu

 David L. Price

Light polarization sensitive photodetectors with m- and r-plane homoepitaxial ZnO/ZnMgO quantum wells

G. Tabares,¹ A. Hierro,^{1,a)} M. Lopez-Ponce,¹ E. Muñoz,¹ B. Vinter,^{2,3} and J.-M. Chauveau^{2,3}

¹ISOM and Dpto. Ingeniería Electrónica, Universidad Politécnica de Madrid, Ciudad Universitaria s/n, 28040 Madrid, Spain

²CRHEA-CNRS, Av. B. Gregory, 06560 Valbonne, France

³University of Nice Sophia Antipolis, Parc Valrose, 06102 Nice cedex 2, France

(Received 22 December 2014; accepted 3 February 2015; published online 12 February 2015)

Homoepitaxial ZnO/(Zn,Mg)O multiple quantum wells (MQWs) grown with m- and r-plane orientations are used to demonstrate Schottky photodiodes sensitive to the polarization state of light. In both orientations, the spectral photoresponse of the MQW photodiodes shows a sharp excitonic absorption edge at 3.48 eV with a very low Urbach tail, allowing the observation of the absorption from the A, B and C excitonic transitions. The absorption edge energy is shifted by ~ 30 and ~ 15 meV for the m- and r-plane MQW photodiodes, respectively, in full agreement with the calculated polarization of the A, B, and C excitonic transitions. The best figures of merit are obtained for the m-plane photodiodes, which present a quantum efficiency of $\sim 11\%$, and a specific detectivity D^* of $\sim 6.4 \times 10^{10}$ cm Hz^{1/2}/W. In these photodiodes, the absorption polarization sensitivity contrast between the two orthogonal in-plane axes yields a maximum value of $(R_{\perp}/R_{\parallel})_{\max} \sim 9.9$ with a narrow bandwidth of ~ 33 meV. © 2015 AIP Publishing LLC.

[<http://dx.doi.org/10.1063/1.4908183>]

The development of ZnO-based optoelectronics in the ultraviolet (UV) is starting to benefit from the recent availability of commercial high quality single crystal ZnO substrates. Using these substrates, which are available in different plane orientations, lattice-matched homoepitaxial layers can be grown with improved characteristics, including lower threading dislocations densities or lower residual carrier concentrations.^{1–3} The use of homoepitaxial layers is probably the most promising path to take full advantage of the high ZnO exciton binding energy for optoelectronic devices. Among these devices, photodetectors with unipolar carrier transport (such as Schottky and metal-semiconductor-metal photodiodes) avoid the inherent difficulties with p-type doping in ZnO,⁴ allowing access to UV photodetection with good figures of merit.^{5–8} Moreover, ZnO has a ternary alloy, (Zn,Mg)O, which can allow tuning the photodetector responsivity to very low wavelengths, below 300 nm with wurtzite structure,^{9,10} as well as increasing the exciton binding energy via the formation of ZnO/(Zn,Mg)O quantum wells (QW). However, the large spontaneous and piezoelectric coefficients in ZnO create large internal built-in electric fields,¹¹ which tend to spatially separate the electron and hole wave functions, resulting in a reduction of the overlap of the wave functions, hindering the benefits of quantum confinement. This problem can be fully overcome by using nonpolar orientations, such as a- and m-plane, where the c-axis lays in-plane and where the electric field along the growth direction is zero.¹ Indeed, ZnO/(Zn,Mg)O QWs with excellent optical and structural characteristics have been demonstrated with homoepitaxy on non-polar ZnO substrates.^{1–3} Besides, in semipolar orientations, such as r-plane where the c-axis forms a given angle with the normal to the growth plane,³ it can be partially reduced. Nonpolar and

semipolar orientations have an additional benefit for certain photodetection applications, because their low crystal symmetry causes a strong optical anisotropy for the excitonic transitions from the three separate p-like valence bands to the s-like conduction band (transitions typically labelled A, B and C excitons). The lowest energy excitonic transitions, A and B, are allowed for light polarization with the electric field (E) perpendicular to the [0001] c-axis, whereas the highest energy transition, C, is essentially allowed for light polarized with E parallel to the c-axis [0001].¹² This sensitivity of the optical absorption coefficient to the polarization state of light can be used to develop light polarization sensitive photodetectors (PSPDs),¹³ without the need of external optical elements, as it has already been demonstrated in a previous work using a-plane ZnO/(Zn,Mg)O QWs.⁵ However, the small differences in the absorption energy of the three excitonic transitions can only be observed if the Urbach tail is very low, i.e., if the crystal quality of the QWs is high. Thus, the use of high quality homoepitaxial layers is the natural path to fabricating PSPDs.

In the present work, we analyze the performance of homoepitaxial ZnO/(Zn,Mg)O multiple quantum well (MQW) UV photodetectors grown on m-plane (polar) and r-plane (semi-polar) ZnO substrates. The high crystal quality of the MQWs allows the observation of the different excitonic absorption transitions from the three valence bands to the conduction band, and thus the photodetectors are evaluated as a function of their sensitivity to the polarization state of the incident light.

Plasma assisted molecular beam epitaxy (MBE) was used to grow (Zn,Mg)O/ZnO homoepitaxial MQWs on m-plane and r-plane ZnO substrates. Details on the homoepitaxial growth can be found in Refs. 1 and 3. The structures contain 10 QWs with a nominal thickness of 1.3 nm, which was chosen in order to minimize the impact of the quantum

^{a)}Email: adrian.hierro@upm.es

confined Stark effect (QCSE) in the r-PSPDs. Indeed, Chauveau *et al.*³ have shown that in semipolar r-plane ZnO/(Zn,Mg)O QWs there exists an internal electric field perpendicular to the QWs with a magnitude of ~ 430 kV/cm. However, the QW thickness of the r-PSPDs used in this study is 1.3 nm, falling in the region where the internal electric field is not able to spatially separate the electron and hole wave-functions. The QWs have (Zn,Mg)O barriers with a Mg concentration of 20 and 25% Mg for the m- and r-plane structures, respectively, and a total (Zn,Mg)O thickness below 250 nm in both orientations, i.e., below the critical thickness.^{1,3} Thus, we can consider both the m- and r-plane ZnO QWs to be strain-free and lattice matched to the ZnO substrate, while the pseudomorphic (Zn,Mg)O barriers to be fully strained. Since the crystal axis orientations determine the allowed optical transitions, it is necessary to correctly define their position in the structures. In m-plane structures, the x, y, and z axes are parallel to the $[1\bar{2}10]$, $[10\bar{1}0]$, and $[0001]$ directions, respectively. On the other hand, in r-plane MQWs, the x' and z' axes are parallel to the $[1\bar{2}10]$, and $[\bar{1}011]$ directions, respectively, and y' is perpendicular to the growth plane. Note that in this latter case, the angle between the c-axis and the growth axis is 42.77° .³

Structures with 10x(Zn,Mg)O/ZnO QWs were used to fabricate Schottky PSPDs with an in-plane geometry. The Schottky contacts consisted of a semitransparent 100 Å-thick Au film, with a co-planar Ti/Al/Ti/Au (200/1000/400/550 Å) extended ohmic contact, which was annealed at 350 °C for 1 min. Prior to the deposition of the Schottky contact, the surface was treated with H₂O₂ during 1 min at 100 °C in order to reduce leakage current in the diodes thanks to the electrical passivation of the surface. The diameter of the Schottky diodes was 200 μm in all cases.

Continuous wave photoluminescence (PL) spectroscopy was performed in both the polar and semipolar structures at low and room temperatures (RTs) using a HeCd laser and a 1 m monochromator (Fig. 1). At low T, the PL spectra of the MQW structures show a rich collection of peaks. In both orientations, the peak at 3.360 eV with a shoulder at 3.375 eV likely corresponds to a donor-bound exciton (D⁰X) and free exciton (FX), respectively, which arise from the ZnO substrate.¹⁴ Looking at the high energy region, two excitonic

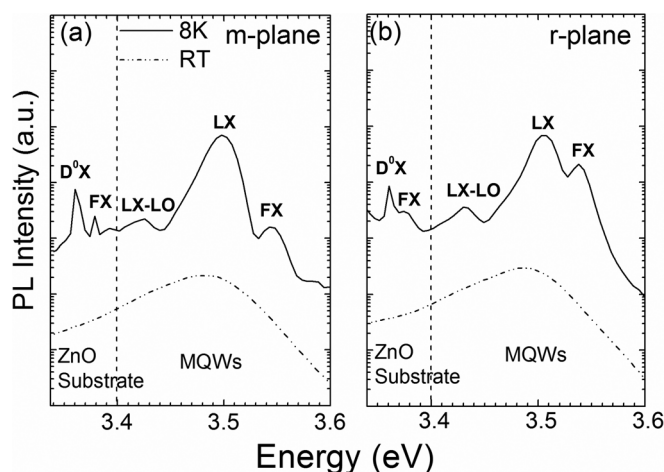


FIG. 1. Unpolarized PL spectra from the m- and r-plane MQWs.

emissions from the MQWs are evident and correspond to the localized exciton (LX) and FX in the QWs.¹⁵ 3.498 and 3.543 eV, for the m-MQWs, and 3.503 and 3.538 eV, for the r-MQWs. The emissions at 3.425 eV (m-plane) and 3.430 eV (r-plane), then correspond to the phonon replica from the QW LX. It is worth mentioning that a recent report on (Zn,Mg)O/ZnO QWs has shown the presence of trions (charged excitons) with a binding energy of ~ 13 meV,¹⁶ whose emission could be related to the one here identified as LX. The excellent agreement between the MQW-FX emission energies for both plane orientations is indicative of the high control over the quantum well thickness along the 10 QWs and in the two different orientations. It also shows that the QCSE does not impact the PL emission energy from the r-plane structures, as expected from their low QW thickness (1.3 nm).³ As shown in Ref. 15, as the temperature is increased, the QW LX emission decreases up to a point where the FX emission dominates. Thus, it is this emission that it is dominant at RT in both MQW structures. It is worth noticing that the overall RT excitonic emission is three times larger in the m-MQWs with respect to the r-MQWs, correlating with the PSPD figures of merit in both structures as discussed below.

The processed photodiodes present excellent electrical rectification characteristics for both MQW structures (inset of Figure 2). In the m-PSPDs, the reverse leakage currents are as low as $\sim 10^{-10}$ – 10^{-11} A/cm² at -2.0 V, with forward bias currents $\sim 10^9$ – 10^{10} times larger at $+2.0$ V. In the r-PSPDs, the rectification ratio is a bit lower, $\sim 10^6$. By fitting the J-V curves with a thermoionic model in the forward region, the ideality factor and Schottky barrier of the m-PSPDs are found to be 1.6 and 1.0 eV, respectively, whereas in the r-PSPDs are 1.9 and 1.1 eV, respectively. The curve bending in the J-V characteristics at forward bias, especially in the r-PSPDs, is indicative of the (Zn,Mg)O influence in the series resistance,¹⁷ and was found to be ~ 36.1 and 3.4×10^3 Ω cm² for m-PSPDs and r-PSPDs, respectively. The spectral response of the PSPDs was measured using a 1/4 m monochromator and a 1000 W Xe lamp as the light source, whereas the responsivity was determined with a calibrated UV-enhanced Si photodiode and a pyrometer. All measurements were performed at room temperature and under steady

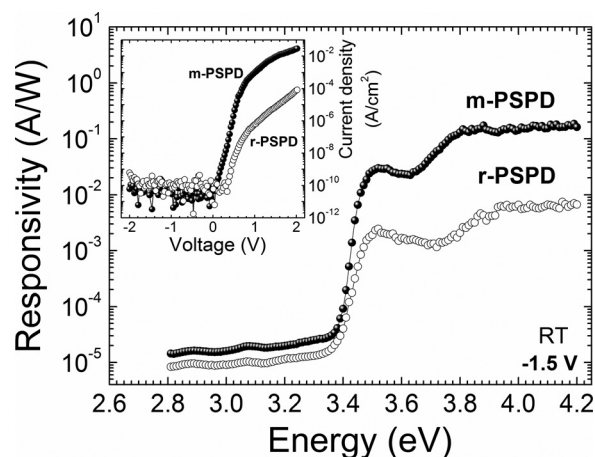


FIG. 2. Spectral response from the m- and r-PSPDs at -1.5 V. The inset shows their J-V characteristics.

state conditions. In order to obtain the absorption energies, the maximum value of the derivative of the photocurrent spectra across the absorption edge was used, approach that accounts well for the transition from Urbach tail to band-to-band absorption.

Figure 2 shows the spectral response under unpolarized light illumination of the photodiodes at -1.5 V, where there are two cut-offs in both detectors. The first one arises from absorption at the QWs and takes place at ~ 3.48 eV, similar for both photodetectors since the QW width is the same and the effect of the slightly different Mg concentration in the barrier is negligible. Indeed, the photocurrent absorption edge is fully consistent with the RT-PL excitonic emission peak, which happens at 3.49 eV in both orientations (Fig. 1). In addition, the photocurrent spectra show a clear peaking shape indicating the strong excitonic nature of the absorption, which results from the high crystal homogeneity of the MQW structures. The second absorption edge at higher energies corresponds to absorption from the (Zn,Mg)O barrier, which occurs at ~ 3.80 and ~ 3.92 eV for the m- and r-PSPDs, respectively.

The spectral response of the m-PSPDs shows some the best reported figures of merits using ZnO-based QWs. The m-PSPDs have a responsivity peak of ~ 30 mA/W, corresponding to a quantum efficiency of $\sim 11\%$, i.e., with no indication of internal gain, as well as a rejection ratio close to $\sim 10^4$. In addition, the absorption edge is very sharp, the entire transition from transparency to absorption happens in only ~ 115 meV, i.e., the Urbach tail is very small. The best reported ZnO-based MQW photodetectors so far have been obtained with a-plane orientations grown on sapphire,⁵ which showed similar responsivities at the same peak energy and bias, but with a transparency-absorption transition around twice as wide (~ 270 meV). In the case of the r-PSPDs, the responsivity is smaller, 2 mA/W, corresponding to a quantum efficiency below 1%, and the rejection ratio is $\sim 10^2$ – 10^3 . The smaller responsivity and rejection ratio with respect to the m-PSPD correlate with the lower PL intensity. Still, the transition from transparency to absorption also happens in a very narrow energy region, ~ 120 meV.

The noise equivalent power (NEP) and the specific detectivity (D^*) have been estimated using the responsivity at -1.5 V and extracting the junction resistance from the reverse bias region of the J-V characteristics in the dark. Without a load, the total shot and thermal noise spectral current densities have been calculated,¹⁸ yielding a NEP = 2.4×10^{-15} W/Hz^{1/2} and a $D^* = 6.4 \times 10^{10}$ cm Hz^{1/2}/W, for the m-PSPD, and a NEP = 4.5×10^{-14} W/Hz^{1/2} and $D^* = 3.5 \times 10^9$ cm Hz^{1/2}/W, for the r-PSPDs. The high values of D^* for the m-MQW photodiodes arises from the very low leakage currents at -1.5 V (~ 2 – 3×10^{-11} A/cm²) and high responsivities achieved. These detectivity values are comparable to those of (Zn,Mg)O-based UV metal-semiconductor-metal photodiodes⁶ or p-n homojunctions in the same spectral region.⁷

The light polarization dependence of the spectral response from the m- and r-PSPDs was also examined under normal incidence conditions, so as to avoid the out of plane polarization component. The incident light was linearly polarized with a UV polarizer. In order to quantify the

sensitivity of the photodiodes to the polarization state of the incident light, two figures of merit can be defined in addition to the responsivity above bandgap.¹⁹ First, the shift in the absorption edge energy (ΔE) obtained from the responsivity when the incident light polarization is rotated 90° between the main in-plane crystallographic axes. Second, the maximum contrast ratio between the responsivities perpendicular and parallel to the main in-plane axes, given by $(R_{\perp}/R_{\parallel})_{\max}$, which determines the polarization sensitivity near the band gap energy. The FWHM of $(R_{\perp}/R_{\parallel})$ yields the polarization-sensitive bandwidth (PSBW). In the case of the m-PSPD, the main in-plane axes are the c- and x-axis. Figure 3 shows the responsivity spectra in the m-PSPD for light linearly polarized parallel ($E_{\parallel c}$) and perpendicular ($E_{\perp c}$) to the c-axis [0001]. We find that when the polarization of the light is rotated by 90° from $E_{\perp c}$ to $E_{\parallel c}$ in the m-plane, the absorption edge is shifted by $\Delta E \sim 30$ meV, indicating a strong dependence of the effective band gap on the polarization state of light (see Table I). This energy shift agrees well with that observed by Matsui and Tabata²⁰ using PL, or with reflectance spectroscopy by Béaur *et al.*,² in strain-free m-plane ZnO QWs. A maximum polarization sensitivity contrast of $(R_{\perp}/R_{\parallel})_{\max} \sim 9.9$ is reached at 3.44 eV (see inset of Figure 3), with a PSBW ~ 33 meV. These figures of merit are better than the ones reported in non-polar a- and m-plane GaN-based PSPDs using bulk layers,^{19,21} where the best reported values are PSBW ~ 73 meV and $(R_{\perp}/R_{\parallel})_{\max} \sim 7$ for m-plane PSPDs.¹⁹ Moreover, they are also better than those previously reported for a-plane PSPDs based on ZnO QWs (PSBW ~ 80 meV and $(R_{\perp}/R_{\parallel})_{\max} \sim 6$).⁵

In the case of the r-PSPDs, the main in-plane orthogonal crystallographic axes are $[\bar{1}210]$ and $[\bar{1}011]$, and the responsivity reveals a shift of the absorption edge of $\Delta E \sim 15$ meV for linearly polarized light with E parallel to these two in-plane directions (Fig. 4). Note that these axes form an angle of 90° . The inset of Fig. 4 shows a maximum polarization sensitivity contrast of $(R_{E_{\perp}[\bar{1}101]}/R_{E_{\parallel}[\bar{1}101]})_{\max} \sim 2.5$, and PSBW of ~ 57 meV at -1.5 V.

In order to identify the origin of the polarization sensitivity of the photodiodes, one must recall that the QWs of the m- and r-PSPDs are strain-free, and thus both the selection rules and oscillator strength components for the excitonic

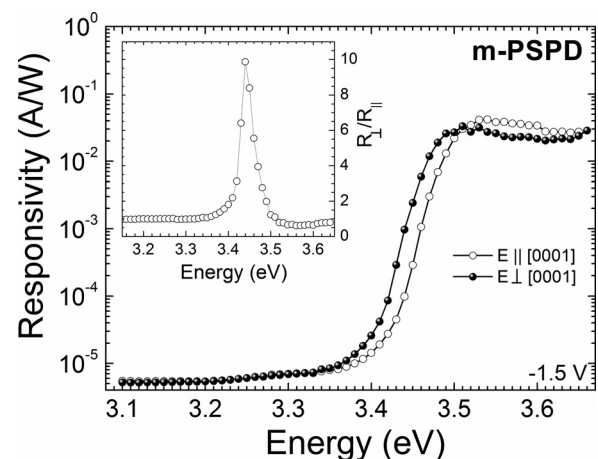
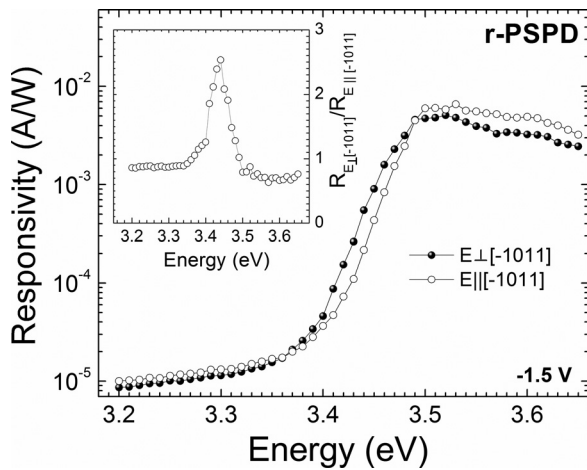


FIG. 3. Spectral response as a function of light polarization for m-PSPD at -1.5 V. The inset shows the $(R_{\perp}/R_{\parallel})$ ratio.

TABLE I. Figures of merit for the polarization-sensitive photodiodes at -1.5 V.

Photodiode	Substrate	$E_{\text{absorption}}$ (eV)	ΔE (meV)	$(R_{\perp}/R_{\parallel})_{\text{max}}$	PSBW (meV)
m-PSPD	m-ZnO	3.470 ($E_{\perp}[\text{0001}]$) 3.500 ($E_{\parallel}[\text{0001}]$)	30	9.9	33
r-PSPD	r-ZnO	3.470 ($E_{\perp}[\bar{1}011]$) 3.485 ($E_{\parallel}[\bar{1}011]$)	15	2.5	57

FIG. 4. Spectral response as a function of light polarization for r-PSPD at -1.5 V. The inset shows the $(R_{E_{\perp}[\bar{1}011]}/R_{E_{\parallel}[\bar{1}011]})$ ratio.

transitions in the QWs should be the same as those from a strain-free ZnO film.¹² In the case of the m-plane MQWs, where the c-axis is found in-plane, one expects to see two dominant excitonic transitions being partially and linearly polarized (A and B) for $E_{\perp}c$, and only one transition which is completely polarized (C) for $E_{\parallel}c$ (see Table II). Note that under normal light incidence conditions, as it is the case, the excitonic transitions corresponding to light polarized parallel to the y-axis are not accessible. Then, according to Table II, illuminating with light polarized parallel to the $[\bar{1}\bar{2}10]$ axis would yield a photocurrent absorption edge where both the A and B excitons contribute equally, whereas illumination with light polarized parallel to $[\bar{1}011]$ would yield absorption only by the C exciton, at 37 meV below that of the A + B absorption. The measured energy shift, $\Delta E \sim 30$ meV, fits well the theoretical values, and thus can be understood to

TABLE II. Calculated A, B, and C excitonic transition energies and their oscillator strength components for the m- and r-PSPDs.

Photodiode	Substrate	Transition	$E_i - E_{i-1}$ (meV)	f_x $[\bar{1}\bar{2}10]$	f_z $[\text{0001}]$
m-PSPD	m-ZnO	A	0	0.5	0
		B	12	0.5	0
		C	37	0	1
Photodiode	Substrate	Transition	$E_i - E_{i-1}$ (meV)	f'_x $[\bar{1}\bar{2}10]$	f'_z $[\bar{1}011]$
r-PSPD	r-ZnO	A	0	0.5	0.27
		B	12	0.5	0.27
		C	37	0	0.46

arise from the contribution of A + B and C for the two orthogonal light polarizations.

The case of r-PSPDs needs a more detailed analysis, since the material is semi-polar and the QCSE could affect the excitonic absorption energies. However, as shown earlier in the PL results, the QW thickness of the r-PSPDs is low enough to minimize the impact of the QCSE. Thus, the observed optical absorption edges in the r-PSPDs are not expected to be affected by the internal electric field. In order to identify the excitonic transitions responsible for the observed sensitivity of the photocurrent to light polarization, we need to recall that the QWs are expected to be strain-free, but the axis orientations are different from those in the m-plane QWs. The oscillator strengths and energies can be obtained by using the values from the excitonic transitions in a-plane strain-free ZnO QWs⁵ and calculating their projections along the new set of coordinate axes in the r-plane (Table II). For polarized light parallel to $[\bar{1}\bar{2}10]$, both the A and B excitonic transitions are allowed with equal probability. However, for polarized light with $E_{\parallel}[\bar{1}011]$, the three excitonic transitions are allowed, although C is significantly more probable than A or B. Weighing the excitonic transition energies by their probability, the average absorption energy for light polarized parallel to $[\bar{1}\bar{2}10]$ should happen at ~ 14 meV above that for light polarized parallel to $[\bar{1}011]$. Looking at the experimental results in Table I, the absorption energy is shifted by $\Delta E \sim 15$ meV, in good agreement with the calculation. Thus, the polarization sensitivity in the r-PSPD arises from the contribution of A + B and A + B + C for the two orthogonal light polarizations.

In summary, we have demonstrated how the use of high quality ZnO/(Zn,Mg)O MQWs homoepitaxially grown on ZnO substrates can allow the development of light polarization sensitive photodetectors. Both nonpolar m-plane and semipolar r-plane PSPDs absorbing at 3.48 eV have been analyzed, and the best results have been obtained with the m-PSPDs, which show excellent figures of merit, including a high quantum efficiency of $\sim 11\%$, a specific detectivity D^* of $\sim 6.4 \times 10^{10}$ cm Hz^{1/2}/W, and a maximum polarization sensitivity contrast of $(R_{\perp}/R_{\parallel})_{\text{max}} \sim 9.9$ with a FWHM of only ~ 33 meV.

The authors would like to acknowledge the financial support from the Spanish Ministry of Economy and Competitiveness (MINECO) through Project Nos. TEC2011-28076-C02-01 and TEC2014-60173-C2-2.

¹J.-M. Chauveau, M. Teisseire, H. Kim-Chauveau, C. Deparis, C. Morhain, and B. Vinter, *Appl. Phys. Lett.* **97**, 081903 (2010).

²L. Béaur, T. Bretagnon, C. Brimont, T. Guillet, B. Gil, D. Tainoff, M. Teisseire, and J.-M. Chauveau, *Appl. Phys. Lett.* **98**, 101913 (2011).

³J.-M. Chauveau, Y. Xia, I. B. Taazaet-Belgacem, M. Teisseire, B. Roland, M. Nemoz, J. Brault, B. Damilano, M. Leroux, and B. Vinter, *Appl. Phys. Lett.* **103**, 262104 (2013).

⁴V. Avrutin, D. J. Silversmith, and H. Morkoc, *Proc. IEEE* **98**, 1269 (2010).

⁵G. Tabares, A. Hierro, B. Vinter, and J.-M. Chauveau, *Appl. Phys. Lett.* **99**, 071108 (2011).

⁶K. W. Liu, J. Y. Zhang, J. G. Ma, D. Y. Jiang, Y. M. Lu, B. Yao, B. H. Li, D. X. Zhao, Z. Z. Zhang, and D. Z. Shen, *J. Phys. D: Appl. Phys.* **40**, 2765–2768 (2007).

⁷K. W. Liu, D. Z. Shen, C. X. Shan, J. Y. Zhang, B. Yao, D. X. Zhao, Y. M. Lu, and X. W. Fan, *Appl. Phys. Lett.* **91**, 201106 (2007).

- ⁸S. Liang, H. Sheng, Y. Liu, Z. Huo, Y. Lu, and H. Shen, *J. Cryst. Growth* **225**, 110 (2001).
- ⁹Y. N. Hou, Z. X. Mei, Z. L. Liu, T. C. Zhang, and X. L. Du, *Appl. Phys. Lett.* **98**, 103506 (2011).
- ¹⁰A. Redondo-Cubero, A. Hierro, J.-M. Chauveau, K. Lorenz, G. Tabares, N. Franco, E. Alves, and E. Muñoz, *Cryst. Eng. Commun.* **14**, 1637 (2012).
- ¹¹C. Morhain, T. Bretagnon, P. Lefebvre, X. Tang, P. Valvin, T. Guillet, B. Gil, T. Taliercio, M. Teisseire-Doninelli, B. Vinter, and C. Deparis, *Phys. Rev. B* **72**, 241305(R) (2005).
- ¹²W. R. L. Lambrecht, A. V. Rodina, S. Limpijumnong, B. Segall, and B. K. Meyer, *Phys. Rev. B* **65**, 075207 (2002).
- ¹³H. T. Grahn, *MRS Bull.* **34**, 341 (2009).
- ¹⁴H. Morkoc and U. Ozgur, *Zinc Oxide: Fundamentals, Materials and Device Technology* (Wiley-VCH, 2009).
- ¹⁵L. Béaur, T. Bretagnon, B. Gil, A. Kavokin, T. Guillet, C. Brimont, D. Tainoff, M. Teisseire, and J.-M. Chauveau, *Phys. Rev. B* **84**, 165312 (2011).
- ¹⁶J. Puls, S. Sadofev, and F. Henneberger, *Phys. Rev. B* **85**, 041307(R) (2012).
- ¹⁷E. Gür, G. Tabares, A. Arehart, J. M. Chauveau, and A. Hierro, *J. Appl. Phys.* **112**, 123709 (2012).
- ¹⁸S. M. Sze and K. K. Ng, *Physics of Semiconductor Devices*, 3rd ed. (John Wiley & Sons, 2007), Chap.13.
- ¹⁹C. Rivera, J. L. Pau, E. Muñoz, P. Misra, O. Brandt, H. T. Grahn, and K. H. Ploog, *Appl. Phys. Lett.* **88**, 213507 (2006).
- ²⁰H. Matsui and H. Tabata, *Appl. Phys. Lett.* **94**, 161907 (2009).
- ²¹A. Navarro, C. Rivera, J. Pereiro, E. Muñoz, B. Imer, S. P. DenBaars, and J. S. Speck, *Appl. Phys. Lett.* **94**, 213512 (2009).